Supporting Information

Thermal ellipsoid plot of 1b. Only the *ipso* carbon atoms of the phenyl groups are shown.

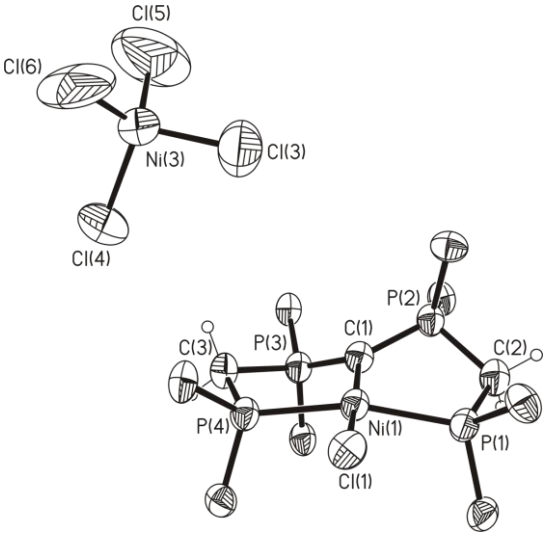

Example for Supramolecular Structure: Compound **7**·2$CHCl_3$

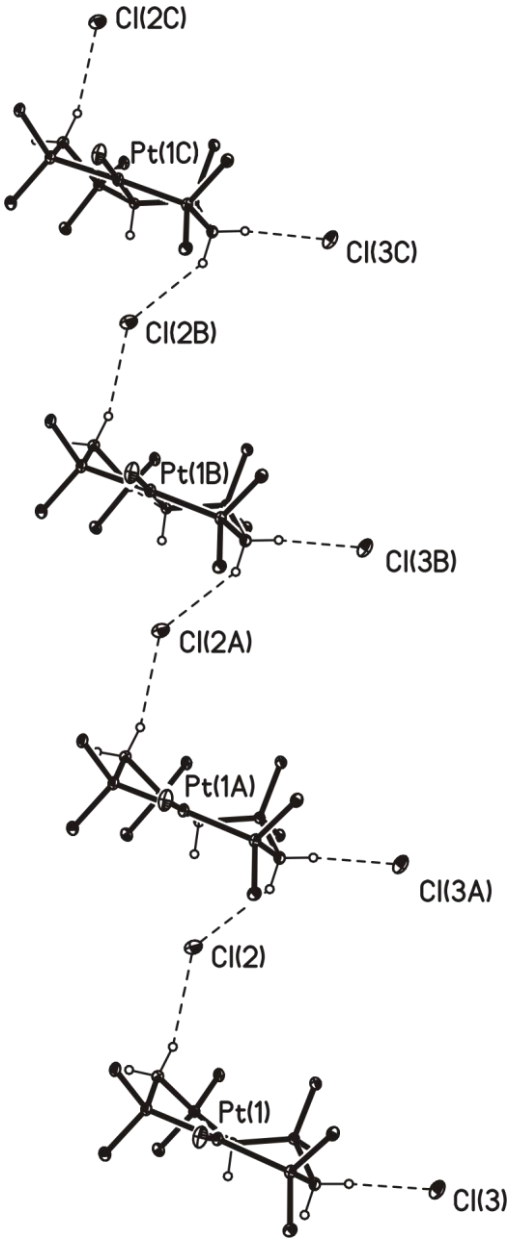

Table 3. Summary of X-ray Data and structure refinement for 1a, 1b, 2 and 3

	1a·$2C_4H_8O_2$	**1b**·CH_2Cl_2	**2**·$2.5C_7H_8$·CH_3OH	**3**·$0.5H_2O$·$2.25C_3H_6O$
formula	$C_{51}H_{44}Cl_2NiP_4$ · 2 $C_4H_8O_2$	$C_{102}H_{88}Cl_6Ni_3P_8$ · CH_2Cl_2	$C_{51}H_{44}Cl_2P_4Pd$ · 2.5 C_7H_8 · CH_3OH	$C_{51}H_{44}Cl_2P_4Pt$ · 0.5 H_2O · 2.25 C_3H_6O
M_r	1086.56	2035.24	1220.42	1186.42
T (K)	233(2)	233(2)	233(2)	233(2)
cryst syst	Orthorhombic	Trigonal	Triclinic	Triclinic
space group	Iba2 (no.45)	$P3_1$ (no.144)	P-1 (no.2)	P-1 (no.2)
a (Å)	9.6018(2)	17.4335(2)	10.2001(2)	9.7629(2)
b (Å)	23.6046(4)	17.4335(2)	12.4004(2)	23.2214(3)
c (Å)	24.3824(4)	31.0829(4)	24.4161(4)	24.4318(4)
α (deg)	90	90	84.068(1)	96.059(1)
β (deg)	90	90	82.649(1)	94.714(1)
γ (deg)	90	120	89.914(1)	92.421(1)
V ($Å^3$)	5526.19(17)	8181.28(17)	3046.28(9)	5482.07(16)
Z	4	3	2	4
D_{calcd} (Mg/m^3)	1.306	1.239	1.331	1.437
μ(mm^{-1})	0.609	0.867	0.540	2.815
F(000)	2272	3144	1266	2396
indep rflns	4807	13390	12411	19002
data / restraints / parameters	4807 / 1 / 319	13390 / 15 / 1129	12411 / 24 / 702	19002 / 48 / 1202
R1 [I>2sigma(I)]	0.0316	0.0630	0.0411	0.0405
wR2 (all data)	0.0727	0.1792	0.1098	0.1034
Largest diff. peak and hole (e.Å-3)	0.253 and -0.213	1.159 and -0.955	0.619 and -0.726	0.930 and -0.822

Table 4. Summary of X-ray Data and structure refinement for 4, 5, 6 and 7

	4·0.5C_7H_8 ·1.5$CHCl_3$	**5**	**6**·3H_2O	**7**·2$CHCl_3$
formula	$C_{51}H_{46}C_{l2}P_4$ · 0.5 C_7H_8 · 1.5 $CHCl_3$	$C_{51}H_{45}ClP_4$	$C_{51}H_{45}Cl_3P_4Pd$ · 3 H_2O	$C_{51}H_{45}Cl_3P_4Pt$ · 2 $CHCl_3$
M_r	1078.78	817.20	1048.55	1321.93
T (K)	233(2)	233(2)	233(2)	233(2)
cryst syst	Orthorhombic	Monoclinic	Triclinic	Triclinic
space group	$P2_12_12$ (no.18)	$P2_1/c$ (no.14)	P-1 (no.2)	P-1 (no.2)
a (Å)	15.2377(6)	16.9190(4)	9.2897(3)	9.4233(2)
b (Å)	20.5124(7)	27.1997(6)	13.5853(6)	15.0455(3)
c (Å)	8.7621(4)	18.7995(2)	19.9199(7)	19.0383(4)
α (deg)	90	90	86.390(2)	90.021(2)
β (deg)	90	92.034(2)	89.649(2)	90.644(2)
γ (deg)	90	90	72.822(2)	96.536(2)
V ($Å^3$)	2738.70(19)	8645.9(3)	2396.84(16)	2681.50(10)
Z	2	8	2	2
D_{calcd} (Mg/m^3)	1.308	1.256	1.453	1.637
μ(mm^{-1})	0.491	0.271	0.730	3.221
F(000)	1116	3424	1076	1312
indep rflns	4284	13577	8354	9424
data / restraints / parameters	4284 / 13 / 323	13577 / 0 / 1017	8354 / 4 / 579	9424 / 13 / 636
R1 [I>2sigma(I)]	0.0498	0.0477	0.0420	0.0367
wR2 (all data)	0.1283	0.1082	0.0813	0.0711
Largest diff. peak and hole	0.594 and -0.267 e.$Å^{-3}$	0.283 and -0.290 e.Å-3	0.587 and -0.593 e.Å-3	0.680 and -0.780 e.Å-3

Detailed description of WIN-DAISY simulation/iteration of NMR spectra

^{31}P-NMR: Simulation and iteration of the $[AX]_2$ system for **5** and **4** was performed by keeping the P1-P4 coupling at 0 Hz. The $[AX]_2$ system of **1a** and **2** was simulated by manual fitting of ^{2}J(P1P4) and ^{2}J(P2P3) to the very weak but detectable outer lines of the respective A and X subspectra (Figure 9), both couplings were kept constant during iteration of ^{2+3}J(P1P2) and ^{3}J(P1P3).

Figure 9. ^{31}P NMR phosphorane region (A-part of the $[AX]_2$ ^{31}P coupling pattern) of [Ni(Cl)(C(dppm)$_2$-κ3P,C,P)]Cl (**1a**): upper trace experimental spectrum, lower trace simulated spectrum showing the (skipped) signals of the intense inner lines (with ^{13}C sattelites at the basis) and the two pairs of weak but detectable outer lines in the very left and right parts of the spectrum, respectively.

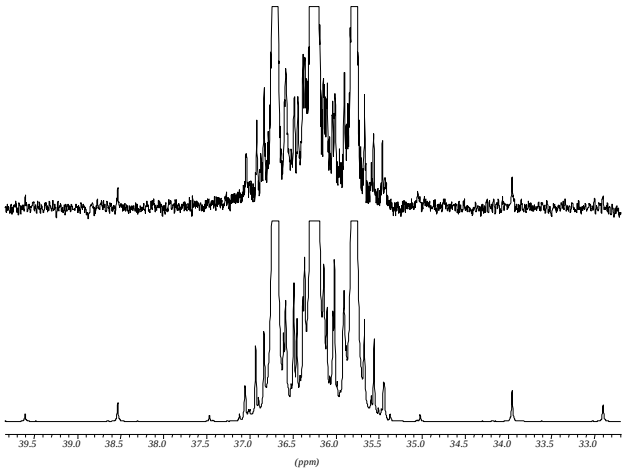

The $[AX]_2$ system of **3**, **6** and **7** was only partly accessible to simulation, since only the N-lines (|J(AX) + J(AX')|) and one single central line of the A and X part, respectively, were resolved. In line with the NMR data for **1a** and **2**, ^{2}J(P1P4) was kept constant at 400 Hz (the spectrum is completely insensitive to variation of this coupling constant between 300 – 500 Hz) and ^{2}J(P2P3) was kept constant at 69 Hz (**3**), -3.7 Hz (**6**) or -1.6 Hz (**7**) (this coupling

constant could be determined from the ^{13}C NMR spectra). $^{2+3}$J(P1P2) and ^{3}J(P1P3) were iterated for **3**, **6** and **7** but show a large uncertainty, due to the featureless triplet structure of the A and X signals. The Pt-P coupling constants were easily accessible from the ^{195}P satellites in the ^{31}P NMR spectrum of the Pt compounds **3** and **7**.

The P-C coupling constants extracted from the ^{13}C NMR spectrum could be verified in the ^{13}C satellites of the ^{31}P signals for all compounds and were found appropriate; only peaks due to the coupling constants larger than ca. 30 Hz were sufficiently separated from the main signals for verification.

^{13}C-NMR: The P-P coupling constants from the ^{31}P spectra were used for simulation of the ^{13}C NMR spectra, P-C coupling constants were fitted manually to the $[AX]_2Z$ (central carbon atom, C1) and AA'XX'Z pattern (all other carbon atoms), respectively, of the ^{13}C signals. Assignment of aromatic carbon resonances was performed by comparison with the literature data for PPh_3, $[MePPh_3]I$ and phosphine complexes.[40b,42] Moreover the assignment of the aromatic carbon signals to Ph1 and Ph2 was unambiguously possible due to the different P-C one bond couplings for C*i* and in general by the significantly different coupling pattern to P1 and P2, respectively, which is largely dependent on the relative magnitudes of $|J(PC) - J(P'C)|$ and $J(PP')$ towards the directly phenyl-bound phosphorus (see also Figure 10):[40] In the free ligands **4** and **5** the C*o*/C*m* signals at P1 show pure doublets, whereas pure triplets are observed for these carbon atoms in all metal complexes. The C*o*/C*m* signals at P2 show pure triplets in **1 - 3** "filled-in doublets" in **6** and **7** and higher order spectra with four to six resolved transitions for **4** and **5**. The C*i* signals show a pattern related to C*o*/C*m* but with further splitting due to substantial ^{3}J(PC) coupling along the ligand backbone, the C*p* signals are either singlets or show only partially resolved splitting. As already mentioned in the ^{31}P NMR section the ^{2}J(P2P3) could be determined unambiguously from the ^{13}C pattern of Ph2-

C*i* for 3 (position of the outer lines of the quintett pattern) or all Ph1a-C*i*/*o*/*m* and Ph1b-C*i*/*o*/*m* signals (intensities of the inner lines of the "filled-in doublets").

Figure 10. ^{13}C NMR aromatic region of [CH(dppm)$_2$]Cl (**5**): upper trace experimental spectrum, lower trace simulated spectrum showing different ^{31}P coupling pattern of C atoms depending of relative magnitudes of $|J(PC) - J(P'C)|$ and $J(PP')$: Singlet (129.9 ppm), doublet (129.1, 133.0 ppm), filled-in doublet (129.4, 133.3 ppm), doublet of filled-in doublets (136.4 ppm), higher order pattern ≥ 4 lines (126.6, 132.4 ppm).

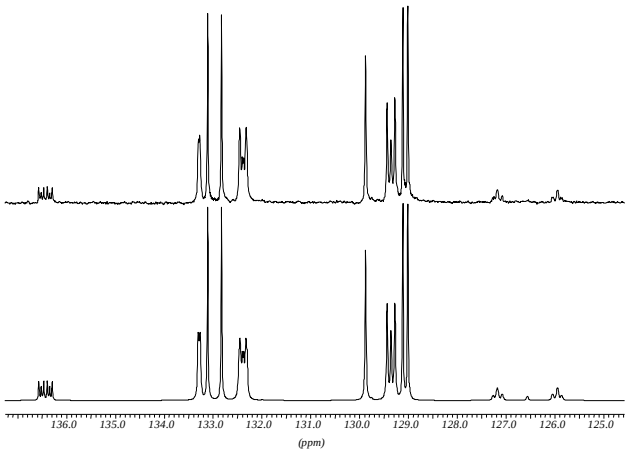

^{1}H NMR: The P-P coupling constants from the ^{31}P NMR spectra were used for simulation of the ^{1}H NMR spectra, H-P coupling constants were fitted manually to the pattern of the ^{1}H signal of H1 and H2. The H2 signals were not accessible for simulation of coupling constants in the free ligands due to an ambiguous pseudo-doublet pattern (**5**) or a featureless, broad appearance ($W_{1/2}$ = 36 Hz; **4**). Only the non-aromatic proton signals were simulated.